Inorganic Chemistry
Article

Inorg. Chem. **2009**, *48*, 6559–6565 **6559**
DOI: 10.1021/ic900478z

Highly Porous Metal-Organic Framework Containing a Novel Organosilicon Linker − A Promising Material for Hydrogen Storage

Stephanie E. Wenzel, Michael Fischer, Frank Hoffmann, and Michael Fröba*

Institute of Inorganic and Applied Chemistry, Department of Chemistry, University of Hamburg, Martin-Luther-King-Platz 6, D-20146 Hamburg, Germany

Received March 11, 2009

The synthesis and characterization of the new metal-organic framework PCN-12-Si (isoreticular to PCN-12) is reported. PCN-12-Si comprises dicopper paddle-wheel units located at the vertices of a cuboctahedron, which are connected by the new linker 5,5′-(dimethylsilanediyl)diisophthalate (dmsdip). The microporous MOF has a high specific surface area of $S_{BET} = 2430\ m^2\ g^{-1}$ and a high specific micropore volume of $V_p = 0.93\ cm^3\ g^{-1}$ ($p/p_0 = 0.18$). The activated form of PCN-12-Si shows a remarkable hydrogen storage capacity. Volumetric low pressure hydrogen physisorption isotherms at 77 K reveal an uptake of 2.6 wt % H_2 at 1 bar. Furthermore, results of theoretical GCMC simulations of hydrogen adsorption are presented. The simulated low pressure isotherm is in excellent agreement with the experimental one. Simulations for the high pressure regime predict an excess hydrogen uptake of 4.8 wt % at 30 bar, which corresponds to an absolute amount adsorbed of 5.5 wt %. In addition, the potential field of H_2 inside PCN-12-Si was derived from the simulations and analyzed in detail, providing valuable insights concerning the preferred adsorption sites on an atomic scale.

Introduction

In recent years metal-organic frameworks (MOFs), which form a new class of ordered organic−inorganic hybrid solids, composed of metal or metal oxide clusters as connectors and organic bridges as linkers, have attracted much attention.[1,2] These compounds have been found to be promising materials for gas storage applications, like CO_2 sequestration, or methane and hydrogen storage. In particular, it is desirable to develop a viable on-board hydrogen storage system for automotives to utilize hydrogen as a clean-burning substitute for fossil fuels.[3] Because of their porous nature and exceptionally high specific surface areas and pore volumes, MOFs have emerged as a potential storage alternative to high-pressure (g-H_2, up to 700 bar) or liquefied hydrogen (l-H_2, temperatures as low as −250 °C are required) tanks, which show several disadvantages in terms of both safety aspects, handling, size of the tank (g-H_2), isolation problems, leakage rates and economic cost (l-H_2). As an adsorbent involving mainly physisorption processes, MOFs are likely superior to technologies based on chemisorption like storage in metal hydrides, as the latter require quite high delivery temperatures.[4]

However, as most of the MOFs are characterized by relatively weak H_2 adsorption energies (typically in the range 4−8 kJ mol^{-1}), hitherto cryogenic temperatures are required to observe significant H_2 uptake.[5,6] To achieve the benchmarks for commercially viable and safe hydrogen storage (the U.S. Department of Energy (DOE) has set the target for on-board hydrogen storage systems as high as 6.0 wt % and 45 g L^{-1} by the year 2010, and 9.0 wt % and 81 g L^{-1} by 2015)[7] at non-cryogenic temperatures there is an immediate need to boost the H_2−framework interactions. Bhatia and Myers predicted an ideal binding energy of 15 kJ mol^{-1} to maximize the amount of adsorbed H_2 attainable at 298 K within the pressure regime 1.5−20 bar.[8] Strategies for improving the H_2 adsorption capacity include (a) decrease of unused pore space, either by tailoring frameworks with very narrow pores through adjustment of the spacer lengths or by making use of framework catenation; in both cases the overlapping potentials from one or more pore walls interacting with the H_2 molecules result in higher binding energies

*To whom correspondence should be addressed. E-mail: michael.froeba@chemie.uni-hamburg.de. Phone: +49-40-42838-3137. Fax: +49-40-42838-6348.

(1) Kitagawa, S.; Kitaura, R.; Noro, S. *Angew. Chem., Int. Ed.* **2004**, *43*, 2334–2375.
(2) Férey, G. *Chem. Soc. Rev.* **2008**, *37*, 191–214.
(3) EERE: Hydrogen, Fuel Cells, & Infrastructure Technologies Program. Homepage, http://www.eere.energy.gov/hydrogenandfuelcells/ (**accessed 2009**).
(4) van den Berg, A. W. C.; Areán, C. O. *Chem. Commun.* **2008**, 668–681.
(5) Collins, D. J.; Zhou, H.-C. *J. Mater. Chem.* **2007**, *17*, 3154–3160.
(6) Zhao, D.; Yuan, D.; Zhou, H.-C. *Energy Environ. Sci.* **2008**, *1*, 222–235.
(7) DOE Office of Energy Efficiency and Renewable Energy Hydrogen, Fuel Cells & Infrastructure Technologies Program Multi-Year Research, Development and Demonstration Plan, available at: http://www.eere.energy.gov/hydrogenandfuelcells/mypp (**accessed 2009**).
(8) Bhatia, S. K.; Myers, A. L. *Langmuir* **2006**, *22*, 1688–1700.

Published on Web 06/16/2009

(values up to 9.5 kJ mol^{-1} have been observed);[9] (b) creation of attractive surface sites within the MOFs via the formation of coordinatively unsaturated metal centers (also called "open metal sites"), typically through the removal of coordinated solvent molecules at the connector nodes.[10−15] Here, isosteric heat of adsorption values (at zero coverage) up to 12.3 kJ/mol have been reported.[16] The most prominent example for unsaturated metal sites probably is the Cu_2 paddle-wheel unit, which is present, for instance, in the MOF $Cu_3(btc)_2$ also known as HKUST-1.[17] Neutron-scattering experiments[18] have verified that H_2 binds at these sites first, most likely through Kubas-type interactions.[19,20] While this approach has been shown to increase H_2 uptake within MOFs appreciably, it is sometimes difficult to synthesize frameworks that can resist collapse upon complete desolvation of metal sites. Furthermore, it is a challenge to introduce a sufficient number of these "open metal sites" to make a practical difference under high loading conditions. Wang and co-workers[21] recently employed an interesting concept to increase the number of nearest neighboring "open metal sites" of each H_2-hosting void in a three-dimensional (3D) framework and to align these sites in a way that they can interact directly with the guests (H_2 molecules) inside the void. The resulting MOF, termed PCN-12 (PCN = porous coordination network), exhibits the highest hydrogen storage capacity at 77 K and 1 bar (3.05 wt %) reported to date. The "open metal sites" are placed at the 12 corners of a cuboctahedron. To realize such cuboctrahedrally caged MOF structures without inducing the formation of NbO-type structures, the linker has to fulfill several structural requirements. In particular, a bent structure between the linked metal sites is favorable, as it is the case for the tetracarboxylate linker 5,5′-methylene-di-isophthalate (mdip).[21]

Here, we report the synthesis of a MOF which is isoreticular to PCN-12, composed of Cu_2 paddle-wheel units connected by the new organosilicon linker 5,5′-(dimethylsilanediyl)diisophthalate (dmsdip). Incorporation of elements with a higher polarizability than carbon is expected to have a positive impact on the binding energy to hydrogen. The MOF has been characterized by means of powder X-ray diffraction measurements, thermal gravimetric analysis (TGA), N_2 physisorption, and modeling techniques. Furthermore, volumetric low pressure hydrogen physisorption data at 77 K are presented as well as Grand-canonical Monte Carlo (GCMC) simulations of hydrogen adsorption.

Experimental Section

Chemicals. Lithium (Fluka, ≥ 99.0%), dichlorodimethylsilane (Merck, ≥ 98.0%), and 1-bromo-3,5-dimethylbenzene (Sigma-Aldrich, 97.0%) were used without further purification. Potassium permanganate (Fluka, ≥ 99.0%), pyridine (Applichem, 99.0%), and *N,N′*-dimethylacetamide (DMA) (Sigma-Aldrich, ≥ 99.5%) were used as obtained.

Synthesis of the Organosilicon Linker. Dimethyl(bis-3,5-dimethylphenyl)silane (1). The synthesis of (**1**) was carried out under argon atmosphere with purified and dried solvents. In a typical synthesis analogous to a literature procedure[22] 25.0 g (0.135 mol) of 1-bromo-3,5-dimethylbenzene were dissolved in 10 mL of diethyl ether and added dropwise to 1.94 g (0.279 mol) lithium granulate in 30 mL diethyl ether at 10 °C . After stirring for 1.5 h at room temperature the reaction mixture was cooled to 0 °C, and 6.95 g (0.0539 mol) of dichlorodimethylsilane in 5 mL of diethyl ether were added dropwise. Afterward, the reaction mixture was stirred for 1.5 h at room temperature. To remove the excess lithium, it was filtrated and ice water was added to the solution. The diethyl ether layer was separated, treated with water, hydrochloric acid (5%), and sodium hydroxide solution (5%), dried over sodium sulfate, and finally the solvent was evaporated to give 14.1 g (0.0526 mol, yield: 98%) of (**1**), a white, crude powder.

^{1}H NMR (400 MHz, $CDCl_3$): δ 0.56 (s, 6 H), 2.35 (s, 12 H), 7.05 (s, 2 H), 7.18 (s, 4 H); ^{13}C NMR (400 MHz, $CDCl_3$): δ −2.20, 21.38, 130.85, 131.87, 137.02, 138.21; IR (film on NaCl): 3015, 2956, 2917, 2857, 1598, 1376, 1268, 1246, 1140, 1038, 869, 844, 811, 792, 771, 697, 677 cm^{-1}.

5,5′-(Dimethylsilanediyl)diisophthalic acid (2). In analogy to a literature procedure,[23] potassium permanganate (50.6 g, 0.392 mol) was added to a solution of 6.80 g (0.0253 mol) of (**1**) in 40 mL of pyridine and 60 mL of water at room temperature. While heating up, a strong exothermic reaction started, and the temperature was kept at 95 °C for 3 h. After removing the excess permanganate by adding methanol, manganese(IV) oxide was removed by filtration. The filtrate was treated with charcoal and acidified with diluted hydrochloric acid to precipitate the raw product (**2**), which was achieved by filtration. To purify the acid, it was dissolved in aqueous sodium carbonate solution, acidified again, filtrated, and dried in vacuum to yield 1.39 g (14%) of (**2**).

^{1}H NMR (200 MHz, DMSO-d_6): δ 0.64 (s, 6 H), 8.23 (d, ^4J = 1.61 Hz, 4 H), 8.46 (t, ^4J = 1.61 Hz, 2 H), 13.30 (s, 4 H); ^{13}C NMR (400 MHz, DMSO-d_6): δ −2.64, 131.27, 131.52, 138.90, 139.04, 167.06; IR (KBr): 2961, 2660, 2546, 1694, 1595, 1473, 1263, 1228, 1170, 1044, 816, 799, 781, 690, 679 cm^{-1}.

Synthesis of the MOF PCN-12-Si. In a typical synthesis, 259 mg (1.07 mmol) of copper(II) nitrate trihydrate and 113 mg (0.291 mmol) of 5,5′-(dimethylsilanediyl)diisophthalic acid were dissolved in 15 mL of DMA. The resulting mixture was placed in a Teflon lined autoclave and heated up to 85 °C with a heating rate of 1 °C min^{-1}. The temperature was held for 46 h before cooling to room temperature with a rate of 5 °C h^{-1}. The resulting blue powder was collected by filtration, washed several times with 15 mL of DMA, and dried in air to yield 156 mg of PCN-12-Si.

Methods. NMR spectra were acquired using a Bruker AVANCE 400 or a Varian Gemini-2000BB spectrometer. Infrared spectra were acquired using a Bruker Vertex 70 FT-IR spectrometer. Powder X-ray diffraction patterns were recorded at room temperature with a STOE STADI P transmission-powder

(9) Dinca, M.; Long, J. R. *J. Am. Chem. Soc.* **2005**, *127*, 9376–9377.
(10) Chen, B.; Ockwig, N. W.; Millward, A. R.; Contreras, D. S.; Yaghi, O. M. *Angew. Chem., Int. Ed.* **2005**, *44*, 4745–4749.
(11) Dinca, M.; Dailly, A.; Liu, Y.; Brown, C. M.; Neumann, D. A.; Long, J. R. *J. Am. Chem. Soc.* **2006**, *128*, 16876–16883.
(12) Forster, P. M.; Eckert, J.; Heiken, B. D.; Parise, J. B.; Yoon, J. W.; Jhung, S. H.; Chang, J. S.; Cheetham, A. K. *J. Am. Chem. Soc.* **2006**, *128*, 16846–16850.
(13) Dinca, M.; Han, W. S.; Liu, Y.; Dailly, A.; Brown, C. M.; Long, J. R. *Angew. Chem., Int. Ed.* **2007**, *46*, 1419–1422.
(14) Georgiev, P. A.; Albinati, A.; Mojet, B. L.; Ollivier, J.; Eckert, J. *J. Am. Chem. Soc.* **2007**, *129*, 8086–8087.
(15) Dinca, M.; Long, J. R. *Angew. Chem., Int. Ed.* **2008**, *36*, 6766–6779.
(16) Chen, B.; Zhao, X.; Putkham, A.; Hong, K.; Lobkovsky, E. B.; Hurtado, E. J.; Fletcher, A. J.; Thomas, K. M. *J. Am. Chem. Soc.* **2008**, *130*, 6411–6423.
(17) Chui, S. S.-Y.; Lo, S. M.-F.; Charmant, J. P. H.; Orpen, A. G.; Williams, I. D. *Science* **1999**, *283*, 1148–1150.
(18) Peterson, V. K.; Liu, Y.; Brown, C. M.; Kepert, C. J. *J. Am. Chem. Soc.* **2006**, *128*, 15578–15579.
(19) Kubas, G. J. *J. Organomet. Chem.* **2001**, *635*, 37–68.
(20) Kubas, G. J. *Chem. Rev.* **2007**, *107*, 4152–4205.
(21) Wang, X.-S.; Shengqian, M.; Forster, P. M.; Daqiang, Y.; Eckert, J.; López, J. J.; Murphy, B. J.; Parise, J. B.; Zhou, H.-C. *Angew. Chem., Int. Ed.* **2008**, *47*, 7263–7266.
(22) Lambert, J. B.; Liu, Z.; Liu, C. *Organometallics* **2008**, *27*, 1464–1469.
(23) Ghatge, N. D.; Jadhav, J. Y. *Synth. React. Inorg., Met.-Org., Chem.* **1984**, *14*, 83–96.

Scheme 1. Synthesis Path of the New Organosilicon Linker 5,5′-(Dimethylsilanediyl)diisophthalic Acid (**2**)

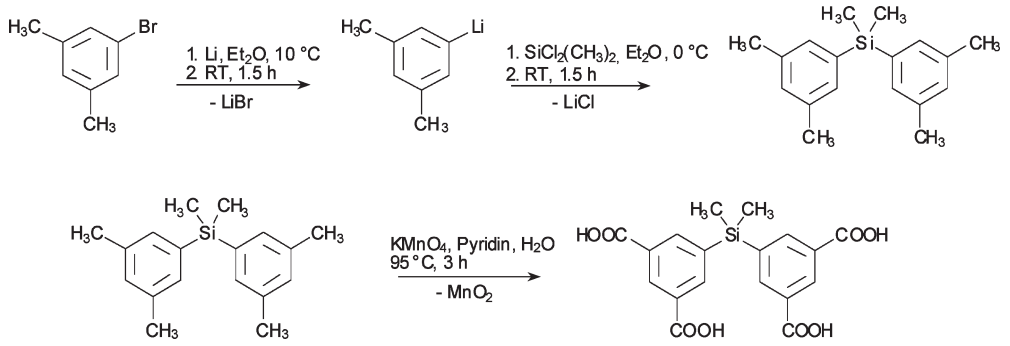

diffractometer using Cu Kα radiation (40 kV, 30 mA; counting time: 70 s; steps: 0.1°(2θ)).

Thermal analysis (thermogravimetry (TG)/mass spectrometry (MS)) was conducted under O_2/argon (20/80) flow (20 mL min^{-1}) with a NETZSCH STA 409 thermobalance coupled by capillary with a Balzers QMG 421 mass spectrometer. The heating rate was 2 °C min^{-1} up to 200 and 5 °C min^{-1} from 200 to 800 °C.

Prior to physisorption measurements all samples were activated in vacuum at 150 °C for 24 h. During the activation process, the samples of PCN-12-Si changed their color from blue to purple; however, the powder X-ray diffraction patterns indicate that the structural integrity is affected only insignificantly (see Supporting Information). Other attempts to activate the material, such as solvent exchange with methanol and dichloromethane as well as activation with supercritical solvent extraction, did not result in samples with higher S_{BET} values or higher hydrogen uptake capacities. In some cases, even the structural order of the frameworks collapsed, resulting in nonporous samples.

Nitrogen physisorption data were recorded with a Quantachrome QUADRASORB-SI-MP at 77 K. The specific surface area was calculated from the adsorption branch in the relative pressure interval from 0.01 to 0.05 using the Brunauer−Emmett−Teller (BET) method. The total pore volume was estimated from the quantity of gas adsorbed at a relative pressure of 0.18.

Volumetric hydrogen physisorption data were recorded at 77 K on a Quantachrome Autosorb 1-MP (purity of helium and hydrogen: 99.999%).

Computational Details. GCMC simulations of the hydrogen adsorption in PCN-12-Si at $T = 77$ K were carried out using the Sorption tool of the Materials Studio package.[24] Dispersive fluid−fluid and fluid−solid interactions were modeled using a Lennard-Jones (LJ) 12−6 potential. The hydrogen molecule was modeled as a single van-der-Waals site (united-atom model), and electrostatic interactions were neglected. To account for the non-negligible quantum effects of hydrogen at low temperatures[25,26] a Feynman−Hibbs correction was applied to the LJ potential[27,28] (for detailed information, see Supporting Information). The LJ parameters of aromatic carbon atoms were adjusted to reproduce theoretical results that were obtained by Heine et al. for the interaction of hydrogen with aromatic systems.[29] The derivation of these parameters will be described in detail elsewhere. The LJ parameters of all other framework atoms were taken from the Universal Force Field (UFF).[30] Lorentz−Berthelot mixing rules were applied to calculate solid-fluid interactions (Supporting Information, Table S-2 summarizes all potential parameters used). The absolute amount adsorbed N_{abs} obtained from the simulation was converted to an excess amount N_{exc} using the following formula: $N_{exc}(p) = N_{abs}(p) - \rho_{H2}(p) \times V_p$. The density of hydrogen at each pressure p was taken from experimental reference data.[31] The pore volume V_p was calculated from GCMC simulations of Helium in PCN-12-Si at room temperature, using appropriately scaled parameters to avoid an overestimation of the He-framework interaction (see Supporting Information).

Results and Discussion

Synthesis. The synthesis of the new non-linear organosilicon tetracarboxylic acid linker (**2**) could be accomplished in a two step reaction, the first step involving a lithium-mediated coupling reaction of 1-bromo-3, 5-dimethylbenzene and dichlorodimethylsilane, while the second step comprised a standard oxidization reaction of the methyl groups of the aromatic cores to the corresponding carboxylic acid groups (Scheme 1). The overall yield was 13.6%. The MOF PCN-12-Si could be obtained by a solvothermal synthesis procedure of copper (II) nitrate trihydrate and (**2**) in DMA. The activation of the as-synthesized form, containing remnant solvent molecules, at elevated temperatures (150 °C, 24 h) leads to a porous compound with "open metal sites".

Structure. Powder X-ray Diffraction and Structure Modeling. The crystal size of the synthesized PCN-12-Si compound was too small to allow for single-crystal X-ray diffraction studies. However, a plausible structure could be obtained by using molecular modeling techniques in conjunction with the comparison to experimental powder X-ray diffraction data. The structure of PCN-12-Si was modeled in analogy to the procedure described by Loiseau et al.,[32] that is, by applying a sort of "homology modeling", using the structure of the original PCN-12 (CCDC entry No. 662918) as a starting point. However, no a priori space group restrictions were applied. First, the methylene groups of the original linker were substituted with the respective dimethylsilylene fragment of the new linker (**2**). After removing any symmetry restrictions,

(24) *Materials Studio*, v4.3; Accelrys Inc: San Diego, CA, 2008.
(25) Tanaka, H.; Kanoh, H.; Yudasaka, M.; Iijima, S.; Kaneko, K. *J. Am. Chem. Soc.* **2005**, *127*, 7511–7516.
(26) Kowalczyk, P.; Gauden, P. A.; Terzyk, A. P.; Bhatia, S. K. *Langmuir* **2007**, *23*, 3666–3672.
(27) Sesé, L. M. *Mol. Phys.* **1994**, *81*, 1297–1312.
(28) Liu, J.; Culp, J. T.; Natesakhawat, S.; Bockrath, B. C.; Zande, B.; Sankar, S. G.; Garberoglio, G.; Johnson, J. K. *J. Phys. Chem. C* **2007**, *111*, 9305–9313.
(29) Heine, T.; Zhechkov, L.; Seifert, G. *Phys. Chem. Chem. Phys.* **2004**, *6*, 980–984.
(30) Rappé, A. K.; Casewit, C. J.; Colwell, K. S.; Goddard, W. A.; Skiff, W. M. *J. Am. Chem. Soc.* **1992**, *114*, 10024–10035.
(31) NIST Chemistry WebBook: NIST Standard Reference Database No. 69, **2005**; http://webbook.nist.gov/chemistry/. (**accessed 2009**)
(32) Loiseau, T.; Mellot-Draznieks, C.; Muguerra, H.; Férey, G.; Haouas, M.; Taulelle, F. *C. R. Chim.* **2005**, *8*, 765–772.

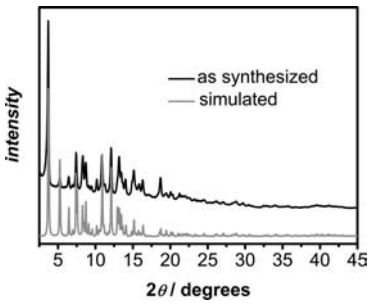

Figure 1. Comparison of the experimental (black) and simulated (gray) powder X-ray diffractograms of PCN-12-Si.

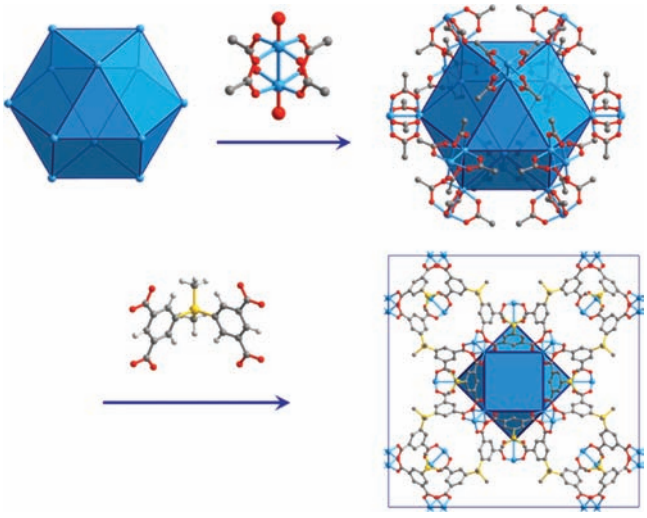

Figure 2. Visualization of the construction principle of PCN-12-Si: Dicopper paddle-wheel motifs form the secondary building units (SBUs) occupying the 12 vertices of a cuboctahedron while 24 isophthalate moieties span all 24 edges. In the lower right panel the whole unit cell is shown, viewed along the *c* direction.

that is, setting the symmetry to *P*1, the constructed model was submitted to a full energy minimization, including optimization of the unit cell dimension and metric, with parameters from the UFF as implemented in Materials Studio 4.3.[24] Van-der-Waals interactions (represented by a classical 12−6 Lennard-Jones potential) beyond 12.5 Å were neglected. The convergence criteria were set to 2.0×10^{-5} kcal mol^{-1} and 0.001 kcal mol^{-1}Å^{-1}, respectively. The geometry optimization converged to result in a plausible tetragonal structure with the space group *P*4/*mmm*, No. 123 ($a = b = 33.7434$ Å, $c = 23.3252$ Å, $\alpha = \beta = \gamma = 90°$, $V = 26{,}558$ Å^3). In Figure 1 the experimental and simulated powder X-ray diffraction patterns are compared. As they show an excellent agreement, it can be confidently assumed that the structure model is correct.

Structure and Pore Description. As PCN-12-Si is an isoreticular compound of PCN-12, the non-linear linker (**2**) also adopts two different conformations: C_{2v}, in which the two phenyl rings face each other, and C_s, in which the two ring planes of the phenyl rings are oriented perpendicular to each other. The linker molecules oriented along the *a* and *b* axis possess the point-group symmetry of C_s, while those oriented along the *c* axis possess C_{2v} symmetry. The construction principle of the PCN-12-Si network is visualized in Figure 2. Dicopper paddle-wheel motifs form the secondary building units (SBUs) occupying the 12 vertices of a cuboctahedron, thereby realizing a "closed packing" of potential "open metal sites", while 24 isophthalate moieties span all 24 edges. Each square face of a cuboctahedron is connected to another square face of a neighboring cuboctahedral cage through four linkers, and every cuboctahedron connects to six others in three orthogonal directions to form a 3D net. In comparison to PCN-12 the unit cell dimensions are slightly larger. This can be easily explained by the fact that the Si−C_{Ph} bond of the linker (**2**) is significantly longer (∼1.85 Å) than the corresponding C_{CH2}-C_{Ph} bond (1.48−1.54 Å) in 5,5′-methylene-di-isophthalate.

A more detailed investigation of the pore geometry reveals that four different types of pores can be distinguished: Cuboctahedral pores at 1/2, 1/2, 1/2 (pore type A), cuboctahedral pores at 0, 0, 1/2 (pore type B), both having approximately a diameter of 12 Å, smaller pores at 1/2, 1/2, 0 and 0, 0, 0 (pore type C, diameter of ∼ 8.5 Å), and finally bigger pores at 1/2, 0, 0 (pore type D, diameter ∼ 13 Å); for a detailed description and additional figures, see Supporting Information, Figures S-6 to S-11.

Hitherto, only very few MOFs with organosilicon linkers are described in the literature, all being structurally different to PCN-12-Si and none of them containing copper as metal ion. Davies and co-workers[33] reported on Zn(II)-containing MOFs based on a series of silicon-centered linkers $(H_3C)_nSi(p\text{-}C_6H_4CO_2H)_{4-n}$ ($n = 0, 1, 2$). These linkers contain tetravalent silicon centers which have been functionalized to give either tetra-, tri-, or dicarboxylic acid derivatives. While the reaction of the tetra-acid with Zn(II) centers gives 3D MOFs, which can be described as an interpenetrating $SrAl_2$ or sra-c net, consisting of tetrahedral silicon-based connectors bridging distorted tetrahedral bimetallic SBUs, the reaction of the tri- or dicarboxylic acids with Zn(II) metal centers give two-dimensional (2D) layered materials.

Furthermore, Lambert et al.[22] obtained MOFs from the reaction of $M(C_6H_4CO_2H)_4$ (M = Si, Ge) with Zn(II). The two structures are quite different from each other, and both are different from that of the already known MOF-36[34] of $C(C_6H_4CO_2H)_4$ with Zn(II). The silicon congener crystallizes in the orthorhombic space group *Pnna* (No. 52), and the zinc portion consists of zinc-oxo chains with two different, alternating zinc atoms. The geometry around one zinc atom is a distorted trigonal bipyramid (five-coordinate), and that around the other is a distorted octahedron (six-coordinate).

Although not containing silicon, a linker which is structurally related to the non-linear linker (**2**) was used by Pan and co-workers.[35] By reaction of 4,4′-(hexafluoroisopropylidene)-bis(benzoic acid) [hfipbb] with Cu(II) nitrate they obtained a 3D interpenetrated framework, containing unique and perfectly ordered microporous one-dimensional (1D) open channels (microtubes) built upon a $Cu_2(hfipbb)_4$ paddle-wheel building unit. Interestingly, while the linker mdip in PCN-12 and dmsdip (**2**) in PCN-12-Si adopts two conformations belonging to the

(33) Davies, R. P.; Less, R. J.; Lickiss, P. D.; Robertson, K.; White, A. J. P. *Inorg. Chem.* **2008**, *47*, 9958–9964.
(34) Kim, J.; Chen, B.; Reineke, T. M.; Li, H.; Eddaoudi, M.; Moler, D. B.; O'Keefe, M.; Yaghi, O. M. *J. Am. Chem. Soc.* **2001**, *123*, 8239–8247.
(35) Pan, J.; Sander, M. B.; Huang, X.; Li, J.; Smith, M.; Bittner, E.; Bockrath, B.; Johnson, J. K. *J. Am. Chem. Soc.* **2004**, *126*, 1308–1309.

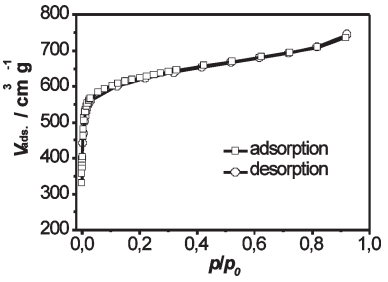

Figure 3. Nitrogen physisorption isotherm (□, adsorption; ○, desorption) of a PCN-12-Si sample, activated for 24 h at 150 °C.

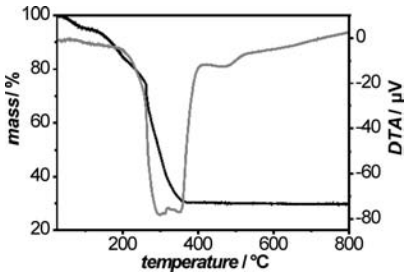

Figure 4. Thermogravimetric analysis (black) and differential thermal analysis (gray) of as-synthesized PCN-12-Si.

point group C_{2v} (the planes defined by the two phenyl rings face each other) and C_s (the planes defined by phenyl rings are oriented perpendicular to each other), respectively, the conformation in hfipbb is in between these extremes and possesses only the symmetry of C_1.

N_2 Physisorption. The nitrogen physisorption measurements show a type-I isotherm (Figure 3) typical of microporous materials. The adsorption and desorption branch are closed; thus, no hysteresis behavior can be inferred. The analysis of the isotherm (according to the criteria of Rouquerol et al.)[36] reveals a specific surface area of S_{BET} = 2430 m^2 g^{-1} (calculated from the adsorption branch in the relative pressure interval from 0.01 to 0.05) and a micropore volume of V_{pore} = 0.93 cm^3 g^{-1} (d < 2 nm; calculated at p/p_0 = 0.18).

Thermal Analysis. The thermal stability of as-synthesized PCN-12-Si was studied using TG-MS and DTA (Figure 4). The overall mass decrease can be roughly divided into three parts: in a first step between 50 and 110 °C, the material shows a mass loss of 5% because of the dehydration of the sample which corresponds to the detected mass of water (m/z = 18). It is followed by a second step, which is accompanied by the detection of DMA (m/z = 87), between 110 and 210 °C. The last weight change, observed in the temperature interval from 210 to 390 °C, generates carbon oxides (CO, m/z = 28; CO_2, m/z = 44) and is caused predominantly by the thermal decomposition of the network. However, DMA is still detected up to 300 °C indicating a delayed desolvation, which slightly overlaps with the thermal decomposition of the material.

Hydrogen Uptake Measurements. Volumetric low pressure hydrogen adsorption at 77 K reveals a remarkable H_2 uptake of 2.6 wt %, at 1 bar (see Figure 5), which

(36) Rouquerol, J.; Llewellyn, P.; Rouquerol, F. In *Characterization of Porous Solids VII*; Lewellyn, P., Rodriguez-Reinoso, F., Rouquerol, J., Seaton, N., Eds.; Elsevier: Amsterdam, *Stud. Surf. Sci. Catal.* 2007, 160, 49−56.

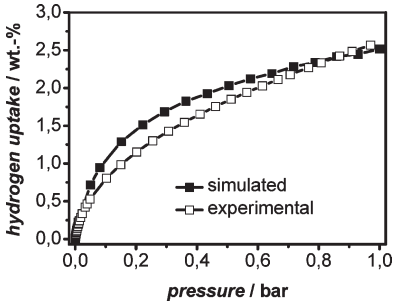

Figure 5. Hydrogen adsorption isotherms of an activated sample (150 °C, 24 h) of PCN-12-Si (□, experimental (volumetric data); ■, data from GCMC simulations).

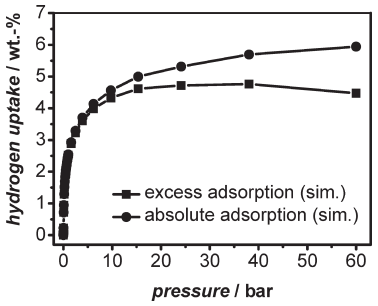

Figure 6. GCMC simulations of the high pressure hydrogen adsorption at T = 77 K of PCN-12-Si (■, excess adsorption; ●; absolute adsorption).

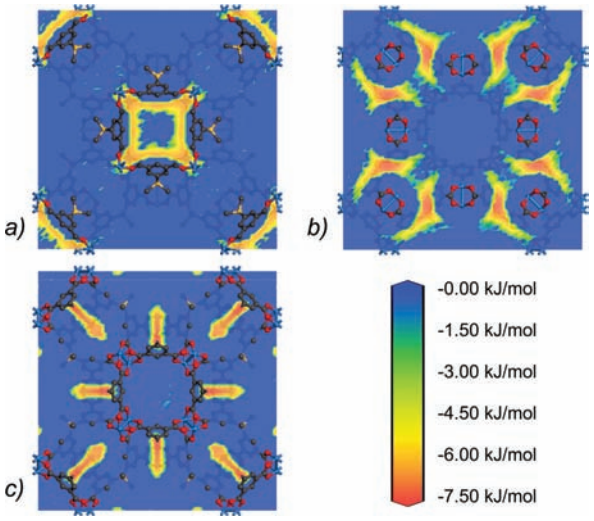

Figure 7. Slices through the calculated potential field: (a) (x, y, 0) slice, (b) (x, y, 1/2) slice, (c) (x, y, 0.717) slice. For clarity, only atoms close to the slices are displayed, and hydrogen atoms are omitted.

ranges among the five highest values reported so far.[21] However, the storage capacity at 1 bar is lower than for the isoreticular material PCN-12. Because of the results of the thermal analysis of PCN-12-Si, one has to consider that activation of the material overlaps with the thermal decomposition, indicated by the detection of DMA (m/z = 87) up to 300 °C. Hence, further studies regarding the activation process of PCN-12-Si are required. Apart from the conventional thermally assisted activation procedure (in this case, at a temperature of 150 °C), we also tried to activate the material by liquid solvent exchange (methanol and dichloromethane) followed by

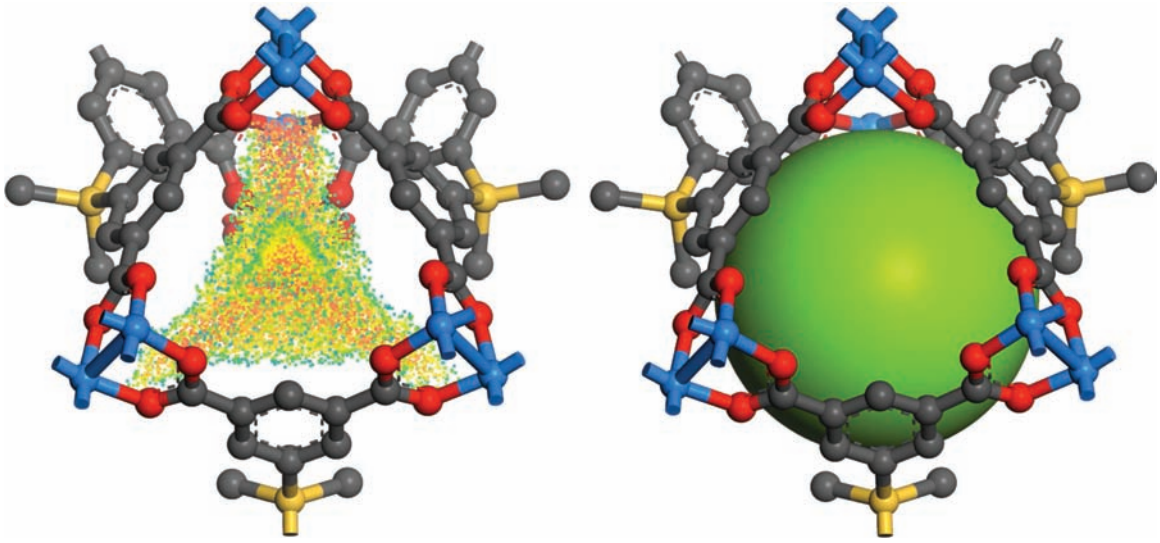

Figure 8. 3D plot of the calculated potential field for a pocket neighboring the pore at (0, 0, 1/2). The same color scheme as in Figure 7 is used, but only field values higher than −2 kJ mol^{-1} are displayed. The figure on the right-hand sized is intended to clarify the geometry of the pocket, using the same representation as in the Supporting Information, Figure S-7.

evacuation at a more moderate temperature as well as by a supercritical activation process[37] with CO_2. Unfortunately, these attempts were not successful, leading to samples which show neither a higher H_2 uptake capacity nor higher S_{BET} values. Further studies concerning a more sophisticated activation protocol are currently under way.

GCMC Simulations. The GCMC simulation of Helium adsorption at room temperature delivers a pore volume of 0.78 cm^3 g^{-1}. This value is smaller than the micropore volume derived from N_2 physisorption measurements (0.93 cm^3 g^{-1}). The Supporting Information, Table S-3 shows that a very similar deviation is observed for PCN-12, while the calculated values for other MOFs are in better agreement with experimental data. These differences are probably caused by particular features of the PCN-12 structure type, which might lead to an increased nitrogen density in the pores.

The agreement between the simulated and experimental hydrogen adsorption isotherm for $T = 77$ K at pressures up to 1 bar, presented in Figure 5, is remarkably good. At higher pressures, the simulation predicts a saturation uptake of approximately 4.8 wt % which is attained in the range of 30 bar (Figure 6). At 60 bar, an absolute amount of 6.0 wt % is reached. In comparison to other Cu-MOFs, the predicted saturation loading of PCN-12-Si ranges well above $Cu_3(btc)_2$[28] and MOF-505 (also termed NOTT-100),[38] which exhibit similar H_2 uptakes at 1 bar. The fact that UMCM-150[39] and NOTT-101, -102, and -103[38] can store somewhat larger amounts of hydrogen at high pressures is clearly related to the larger pore volume of these compounds.

Furthermore, the GCMC simulations deliver the isosteric heat of adsorption q_{st}. The calculated values of q_{st} are plotted for H_2 loadings up to 4.5 wt % (corresponding to pressures up to 10 bar) in the Supporting Information, Figure S-3. The q_{st} value extrapolated to zero loading amounts to 6.7 kJ mol^{-1}, which is very similar to experimental values obtained for other Cu-MOFs, such as $Cu_3(btc)_2$ (6.8 kJ mol^{-1}),[40] NOTT-100 to NOTT-107 (5.3−6.7 kJ mol^{-1}),[38] or UMCM-150 (7.3 kJ mol^{-1}).[39] In contrast to most of these compounds, the q_{st} values of PCN-12-Si decrease only slightly upon increasing hydrogen loading, exceeding 5.5 kJ mol^{-1} even when saturation is nearly attained.

Sparked by this interesting observation, we investigated the adsorption positions in more detail using the H_2 potential field resulting from the GCMC simulations. Because fluid−fluid interactions will increasingly influence the potential field upon increasing pressure, the field derived from a calculation at low pressure ($p = 0.1$ bar) was studied. Three slices where cut through the potential field in an orientation perpendicular to the *c*-axis at different *z*-coordinates (Figure 7 a−c).

The (x, y, 0) slice shows areas of high interaction potential within the small cuboctahedral pores at the origin (pore type C) and the (a,b) face of the unit cell. The highest potential values (approximately −6.4 kJ mol^{-1}) are reached at the faces of the cuboctahedra, which are closely surrounded by two Cu_2 paddle-wheels and two Si atoms. In the (x, y, 1/2) slice, regions of even higher potential (approximately −7.1 kJ mol^{-1}) are visible. They correspond to the pockets adjacent to the central cuboctahedral pores (pore type A), which have two paddle-wheels, four benzene rings, and two Si atoms in their direct environment. The (x, y, 0.717) slice shows confined areas of similar interaction strength. They correspond to pockets, which are neighboring the large pores centered at (1/2, 0, 0) (pore type D), and the cuboctahedral pores centered at (0, 0, 1/2) (pore type B), respectively. The former are surrounded by two paddle-wheels and three benzene rings. Concerning the latter, a 3D plot

(37) Nelson, A. P.; Farha, O. K.; Mulfort, K. L.; Hupp, J. T. *J. Am. Chem. Soc.* **2009**, *131*, 458–460.
(38) Lin, X.; Telepeni, I.; Blake, A. J.; Dailly, A.; Brown, C. M.; Simmons, J. M.; Zoppi, M.; Walker, G. S.; Thomas, K. M.; Mays, T. J.; Hubberstey, P.; Champness, N. R.; Schröder, M. *J. Am. Chem. Soc.* **2009**, *131*, 2159–2171.
(39) Wong-Foy, A. G.; Lebel, O.; Matzger, A. J. *J. Am. Chem. Soc.* **2007**, *129*, 15740–15741.
(40) Rowsell, J. L. C.; Yaghi, O. M. *J. Am. Chem. Soc.* **2006**, *128*, 1304–1315.

of the potential field is shown in Figure 8. The plot reveals that a relatively strong interaction is present throughout the pore, the highest potential being reached in the central regions, which are located at equal distance to several paddle-wheels, benzene rings, and/or Si atoms.

The study of the potential field shows that the favorable hydrogen adsorption properties of PCN-12-Si can be directly related to the presence of voids of relatively small diameter (pores and pockets < 9 Å) in the structure. The value of the potential field can reach up to -7 kJ mol^{-1} in these small voids because several framework atoms contribute considerably to the total solid-fluid interaction energy. Since there are numerous small voids per unit cell, with each of these voids being able to accommodate several H_2 molecules, the relatively high heat of adsorption of this compound, even at high hydrogen loadings, can be understood from these observations, too.

Conclusions

It has already been discussed that the presence of unsaturated metal sites could be a possible route to create MOFs with high hydrogen adsorption enthalpies. The original PCN-12 structure was designed as a close packing of open Cu sites. Short metal-H_2 distances and relatively high interaction strengths at open metal sites, which have been observed experimentally, for instance, in $Cu_3(btc)_2$,[18,41] indicate that the adsorption at these sites is not dominated by dispersive interactions. Therefore, it is obvious that no adsorption at these sites is predicted from the GCMC simulations, which are based solely on van-der-Waals interactions. The fact that the simulation is in very good agreement with experimental data in spite of this shortcoming, together with the observation that DMA is still present in the structure after exposing the sample to the activation temperature, indicate that PCN-12-Si could not be activated completely. This would also explain the reduced uptake of PCN-12-Si with respect to PCN-12, particularly at very low pressures.

However, it should not be overlooked that the adsorption at the "open metal sites" cannot account for more than 0.78 wt % in PCN-12-Si (or 0.86 wt % in the original PCN-12), assuming maximal activation and one adsorbed hydrogen molecule per Cu site.[42] While it seems reasonable to attribute part of the exceptionally high hydrogen uptake of PCN-12 at 1 bar to adsorption at these sites, there must be other favorable factors. The simulations presented here for the isostructural compound PCN-12-Si show that the particular arrangement of the non-linear linker (**2**) between the Cu_2 paddle-wheels leads to a formation of numerous small voids with high adsorption potential. Thus, the PCN-12 structure type combines both approaches which are intended to increase the hydrogen adsorption enthalpy, namely, (a) tailoring frameworks, in which overlapping potentials from one or more pore walls with interacting H_2 molecules result in higher binding energies and (b) creating attractive surface sites within the MOFs via the formation of "open metal sites".

The development of a more efficient and complete activation procedure, as well as investigations on the importance of the presence of the silylene group in PCN-12-Si instead of the methylene group in PCN-12, for instance, in terms of polarizability and effects on the specific surface area, is currently under way.

Acknowledgment. We thank the BMBF (Project "Nanosorb", FKZ: 03X0011C) and the FCI (*Fonds der Chemischen Industrie*) for financial support, Carsten Menke from Accelrys, Inc. for guidance concerning Materials Studio, Quantachrome, Inc. for the hydrogen adsorption measurements, and Inga Piller for assistance during the synthesis of the linker.

Supporting Information Available: (1) Comparison of the P-XRD patterns of as-synthesized and activated samples of PCN-12-Si as well as of the simulated pattern (2) experimental low-pressure hydrogen adsorption data, (3) table with the unit cell metric and atomic coordinates of the structural model of PCN-12-Si, (4) derivation of H_2 parameters, (5) table of force-field parameters, (6) calculation of the pore volume, (7) hydrogen adsorption data of GCMC simulations, (8) calculated values of isosteric heat of hydrogen adsorption, (9) calculated hydrogen adsorption isotherm for PCN-12 (10) description of the different pore types in PCN-12-Si. This material is available free of charge via the Internet at http://pubs.acs.org.

(41) Vitillo, J. G.; Regli, L.; Chavan, S.; Ricchiardi, G.; Spoto, G.; Dietzel, P. D. C.; Bordiga, S.; Zecchina, A. *J. Am. Chem. Soc.* **2008**, *130*, 8386–8396.

(42) GCMC simulations for PCN-12 using the same parameters deliver a hydrogen uptake of 2.2 wt % at $p = 1$ bar, while the experimental value amounts to 3.05 wt %. This underestimation is in line with the statement that the interaction of hydrogen with the unsaturated metal sites is not accounted for in the simulations, and vice versa, the good agreement observed for PCN-12-Si reflects the incomplete activation of the metal sites in this system. If a complete activation of the metal sites was possible for PCN-12-Si, an uptake of well above 3 wt % at 1 bar could be expected. The simulated isotherms for PCN-12 are shown in Supporting Information, Figures S-4 and S-5.